7th International Building Physics Conference

IBPC2018

Proceedings

SYRACUSE, NY, USA

September 23 - 26, 2018

Healthy, Intelligent and Resilient Buildings and Urban Environments

ibpc2018.org | #ibpc2018

Experimental analysis of micro-cracks on the change of moisture transport properties of AAC

Jiří Maděra[1,*], Jan Kočí[1], Václav Kočí[1], Miloš Jerman[1], Magdaléna Doleželová[1]

[1]Czech Technical University in Prague, Czech Republic

[*]*Corresponding email: madera@fsv.cvut.cz*

ABSTRACT
In this paper, series of experiment measurements is carried out in order to study effect of freeze/thaw loading on the change of moisture transport properties of autoclaved aerated concrete. The samples were subjected to 15, 30 and 45 freeze/thaw cycles and subsequently basic physical properties, pore size distribution and water vapor and liquid water transport properties were investigated. The results showed significant changes in material properties of the material. The results of this research can be further implemented into computational models in order to bring the simulation results closer to the reality.

KEYWORDS
Autoclaved aerated concrete, freeze/thaw cycles, moisture transport properties, damage

INTRODUCTION
The effects of natural environment, such as air temperature, relative humidity, and solar and wind factors always vary in time, acting on the surface of building materials. Such effects may cause biological, chemical, or physical degradation of the material (Bertron, 2014; Kordatos et al., 2013; Sandrolini et al., 2007). When the materials are exposed to low temperatures, the ice damage needs to be considered in the first place. It is initiated through the nucleation, growth and interaction of micro-cracks, which usually occur internally. Such processes are manifested by volume expansion during cooling and by macroscopic cracks that develop after repeated cycles of freezing and thawing. (Beaudoin and MacInnis, 1972; Powers and Helmuth, 1953)

The ice damage is usually observed and investigated from a structural or esthetic point of view as usually strength loss of the material, surface cracks or detachment of renders are of interest. However, there exist some additional effects of ice damage, which are not apparent at a first glance. For example, building materials subjected to freeze-thaw loading become more permeable for the liquid water and water vapor due to the presence of micro- and macro-cracks in their structure. For that reason those materials become more vulnerable for the rest of their service life. Therefore, the freeze-thaw effects should be investigated also in this manner in order to analyze the effect of cracks on the change of moisture transport properties of building materials and to increase the credibility of service life analyses.

In this paper a series of experiments is conducted in order to investigate moisture transport properties of autoclaved aerated concrete after repeated freeze-thaw loading. The samples are fully saturated and subjected to different number of freeze-thaw cycles. Then, after drying process, for each sample the moisture transport properties, namely water vapor diffusion resistance factor and apparent moisture diffusivity, are determined and their dependence on the number of freeze-thaw cycles is investigated and discussed.

MATERIALS AND METHODS

Studied material

For the investigation of the effect of micro-cracks on the change of moisture transport properties, an autoclaved aerated concrete (AAC) P1.8-300 produced by company Xella was selected. Its basic physical, thermal and hygric properties (Jerman et al., 2013; Maděra et al., 2017) are shown in Table 1.

Table 1. Basic physical, thermal and hygric properties of studied AAC.

Parameter	Unit
Bulk density ρ (kg/m^3)	289
Open porosity ψ (%)	86.9
Specific heat capacity c (J/kg/K)	1090
Water vapor diffusion resistance factor μ_{dry} (-)	15.61
Water vapor diffusion resistance factor μ_{sat} (-)	6.17
Thermal conductivity λ_{dry} (W/m/K)	0.071
Thermal conductivity λ_{sat} (W/m/K)	0.548
Apparent moisture diffusivity κ (m^2/s)	7.02 10^{-8}

For the further laboratory testing, the material was cut and different sets of samples having specific dimensions were prepared. For the measurement of apparent moisture diffusivity, rectangular prismatic specimens with the dimensions of 20 mm x 40 mm x 300 mm were prepared. The water vapor diffusion resistance factor was measured on block samples with the dimensions 100 mm x 100 mm and height of 20 mm (see Fig. 1), which were cut from the original AAC block.

Figure 1. AAC samples for measurement of water vapor resistance diffusion factor.

Experimental methods

The prepared samples were subjected to the freeze/thaw loading similarly to freeze resistance tests defined by ČSN EN 15304 (2010). First, the samples were dried, then submerged in water for 48 hours and left for another 24 hours in the laboratory in polyethylene bags to reach moisture content equilibration. After that, each sample was loaded by 15, 30 or 45 freeze/thaw cycles in order to create various amount of micro-cracks inside the material. Freezing period

was realized for 8 hours at -15 °C, thawing period 8 hours at 20 °C. The samples loaded by defined number of freeze/thaw cycles were then subjected to particular measurement of water vapor and liquid moisture transport properties. Simultaneously, the pore size distribution function of loaded samples was determined in order to provide preliminary information on changes in material's pore structure.

The apparent moisture diffusivity was obtained through the measurement of water absorption coefficient. The water absorption coefficient was determined by free water intake experiment. The cumulative mass of water in terms of the square-root-of-time rule commonly employed in the diffusion theory (Crank, 1975) can be expressed as

$$i = A \cdot t^{1/2}, \tag{1}$$

where i (kg·m^{-2}) is the cumulative mass of water and A (kg·m^{-2}·s$^{-1/2}$) is the water absorption coefficient. Once A is known, the apparent moisture diffusivity can be calculated according to basic formula given by Kumaran (1999)

$$\kappa_{app} \approx \left(\frac{A}{w_{sat} - w_0} \right)^2, \tag{2}$$

where κ_{app} (m^2·s^{-1}) is the apparent moisture diffusivity, w_{sat} (kg·m^{-3}) is the saturated moisture content and w_0 (kg·m^{-3}) is the initial moisture content.

The water vapor transport properties were determined by means of water vapor diffusion resistance factor. For that reason the cup method was employed (Roels et al., 2004), which is the most frequently used in the practice. The method, defined by ISO (EN ISO 12572, 2001), is based on one-dimensional water vapor diffusion where the diffusion water vapor flux through the specimen and partial water vapor pressure in the air under and above specific specimen surface are measured. Water vapor transition properties of the investigated material are found by placing a specimen on the top of a cup and sealing it. The water vapor diffusion permeability δ (s) is calculated from the measured data according following equation

$$\delta = \frac{\Delta m \cdot d}{S \cdot \tau \cdot \Delta p_p}, \tag{3}$$

where Δm (kg) is the amount of water vapor diffused through the sample, d (m) is the sample thickness, S (m^2) is the specimen surface, τ (s) is the period of time corresponding to the transport of mass of water Δm, and Δp_p (Pa) is the difference between partial water vapor pressure in the air under and above specific specimen surface. Once the water vapor diffusion permeability is known, the water vapor diffusion resistance factor μ (-) can be calculated through water vapor diffusion coefficient D (m^2·s^{-1}) as

$$D = \frac{\delta \cdot R \cdot T}{M}, \tag{4}$$

$$\mu = \frac{D_a}{D}, \tag{5}$$

where R (kg·m^2·s^{-2}·K^{-1}·mol^{-1}) is the universal gas constant, M (kg·mol^{-1}) is the molar mass of water, T (K) is the absolute temperature, and D_a (m^2·s^{-1}) is the diffusion coefficient of water vapor in the air.

The pore size distribution function was determined using two different approaches. The distribution of pores up to 10 μm was determined using mercury intrusion porosimetry, while the amount of larger pores was calculated from total open porosity obtained by helium pycnometry.

RESULTS

Following data were obtained using experimental methods described in previous section. The basic physical properties such as bulk density, matrix density and open porosity are shown in Table 2. The distribution of pores is shown in Fig. 2.

Table 2. Basic physical properties of AAC

Sample	Matrix density ρ_{mat} (kg·m^{-3})	Bulk density ρ (kg·m^{-3})	Open porosity ψ (%)
unloaded (reference)	2034.0 ± 40.7	289.0 ± 4.3	85.1 ± 2.8
15 F/T cycles	2060.4 ± 41.2	281.7± 4.2	86.4 ± 2.9
30 F/T cycles	2016.1 ± 40.3	292.5 ± 4.4	85.5 ± 2.8
45 F/T cycles	2005.8 ± 40.1	285.0 ± 4.3	85.8 ± 2.8

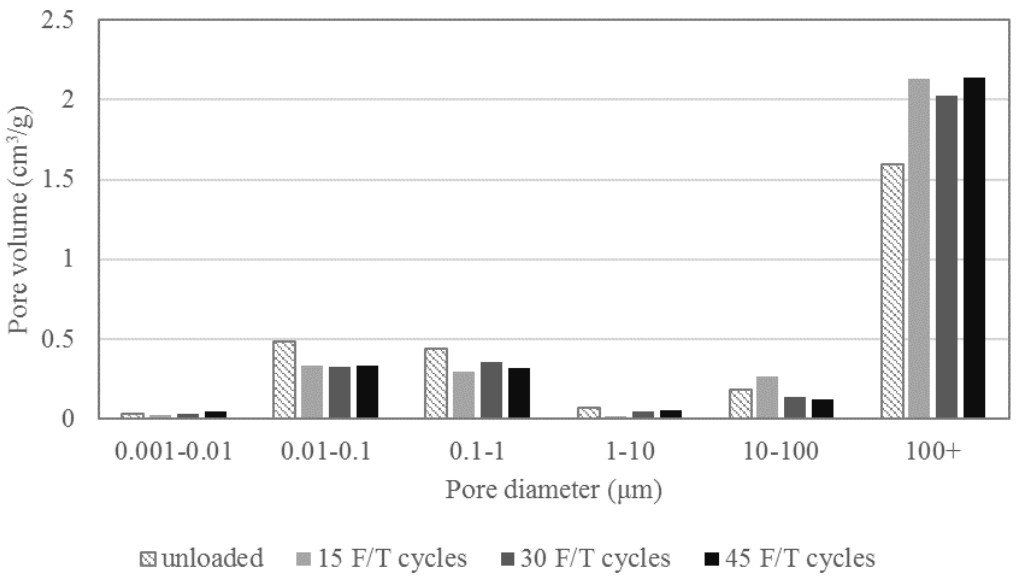

Figure 2. Pore size distribution of studied AAC

The measured water vapor and liquid water transport parameters are shown in Table 3.

Table 3. Water vapor and liquid water transport properties

Sample	Water vapor diffusion resistance factor μ (-)	Water absorption coefficient A (kg·m^{-2}·s$^{-1/2}$)	Apparent moisture diffusivity κ_{app} (m^2·s^{-1})
unloaded (reference)	15.6 ± 2.3	0.106 ± 0.005	(7.020 ± 0.351) · 10^{-8}
15 F/T cycles	5.7 ± 0.9	0.021 ± 0.001	(2.652 ± 0.133) · 10^{-9}
30 F/T cycles	6.4 ± 1.0	0.020 ± 0.001	(2.450 ± 0.123) · 10^{-9}
45 F/T cycles	6.5 ± 1.0	0.019 ± 0.001	(2.139 ± 0.107) · 10^{-9}

DISCUSSION

The presented results clearly show the change in material parameters of the sample before and after loading by certain numbers of freeze/thaw cycles. When basic physical properties are taken into account, it is obvious that freeze/thaw cycles generated some micro-cracks inside the material manifested by slight decrease of bulk density. However, the change is withing the frame of measurement error. The increase of bulk density for the sample loaded by 30 freeze/thaw cycles can be explained by inhomogeneity of the original block from which the samples were cut. In the same way, the total porosity slightly increased. The changes of materials pore structure are evident from Fig. 2, where the amount of largest pores increased with the freeze/thaw loading.

The change of material structure affected the water vapor and liquid water transport properties. When water vapor diffusion resistance factor is discussed, it is evident that the material became more permeable for the water vapor. The values significantly decreased, however it seems that the number of freeze/thaw cycles does not have significant influence on the value change. Therefore, it can be concluded that major changes in material's pore structure appear after 1 to 15 freeze/thaw cycles and the additional loading does not affect the structure in significant way. In order to evaluate the critical number of freeze/thaw cycle that causes substantial change of material's structure, some additional testing should be performed with finer scale such as 1 or 2 freeze/thaw cycles.

The determination of water adsorption coefficient and apparent moisture diffusivity of AAC was very difficult. Basically, the reason for this is a coarse pore structure of the material making the gravity forces an important factor. With increasing pores in the material the absorption coefficient and apparent moisture diffusivity decreases. However, in order to provide more representative view on liquid moisture transport properties of studied material, another series of experiment needs to be conducted. The objective is to eliminate the effect of gravity forces and therefore the experiment should be designed to simulate moisture transport in horizontal position instead of vertical one.

Also, the cooling of material was done for -15 °C according to national standard, however, this temperature might not be sufficient enough. Using the Gibbs-Thompson equation for calculation of freezing point depression in the pores, the size of largest pore where the freezing occur may be calculated as

$$R = \frac{2T_0\gamma_{sl}v_l}{\Delta h_b \Delta T_f}, \tag{6}$$

where γ_{sl} (mJ·m^{-2}) is the surface free energy (interfacial tension) of the solid/liquid interface (γ_{sl} = 31.7 ± 2.7 mJ·m^{-2}), v_l (cm^3·mol^{-1}) the molar volume of the liquid (v_l = 18.02 cm^3·mol^{-1}), and Δh_b (kJ·mol^{-1}) the melting enthalpy in the unconfined (bulk) state (Δh_b = 6.01 kJ·mol^{-1}), all quantities taken at the bulk coexistence temperature T_0 (T_0 = 273.15 K). ΔT_f (K) is the freezing temperature, i.e. $\Delta T_f = T_0 - T_{cooling}$. Based on Eq. (6), the largest pore with affected by freezing has a diameter of approximately 0.02 μm. For that reason, it will be suggested in further experiments to decrease the freezing temperature to at least -30 °C in order to affect the smallest pores (up to 0.008 μm) by ice damage.

CONCLUSIONS

The water vapor and liquid water transport properties of the autoclaved aerated concrete were investigated in this paper. The samples were first loaded by various number of freeze/thaw cycles in order to induce ice damage to the material. Then, basic physical properties, pore size distribution and moisture transport properties were analyzed. The results proved significant

change in water vapor transport properties as the material become more permeable for the water vapor. The liquid water transport properties described by apparent moisture diffusivity decreased after loading by freeze/thaw cycles. However, the methodology for vertical water uptake was found not suitable for this kind of material due to significant effect of gravity forces. The analysis of pore size distribution revealed significant changes in pore structure of the material supporting the conclusions made in this paper.

ACKNOWLEDGEMENTS

This research has been financially supported by the Czech Science Foundation, under project No 17-01365S.

REFERENCES

Beaudoin J.J. and MacInnis, C. 1972. The mechanism of frost damage in hardened cement paste. *Cement and Concrete Research*, 4, 139-147.

Bertron A. 2014. Understanding interactions between cementitious materials and microorganisms: a key to sustainable and safe concrete structures in various contexts. *Materials and Structures*, 47(11), 1787-1806.

Crank J. 1975. *The Mathematics of Diffusion*. Oxford: Clarendon Press.

ČSN EN 15304. 2010. Determination of the freeze-thaw resistance of autoclaved aerated concrete. Czech Office for Standards, Metrology and Testing, Prague.

EN ISO 12572. 2001. Hygrothermal performance of building materials and products. Determination of water vapor transmission properties. The European Committee for standardization, Brussels.

Jerman M., Keppert M, Výborný J., and Černý R. 2013. Hygric, thermal and durability properties of autoclaved aerated concrete. *Construction and Building Materials*, 41(1), 352-359.

Kordatos E.Z., Exarchos D.A., Stavrakos C., Moropoulou A., and Matikas T.E. 2013. Infrared thermographic inspection of murals and characterization of degradation in historic monuments. *Construction and Building Materials*, 48, 1261-1265.

Kumaran M.K. 1999. Moisture diffusivity of building materials from water absorption measurements. *Journal of Thermal Envelope and Building Science*, 22, 349-355.

Maděra J., Kočí V., Doleželová M., Čáchová M., Jerman M., and Černý R. 2017. Influence of weather-affected material characteristics on appearance of freeze/thaw cycles in building envelopes. *AIP Conference Proceedings*, 1866, 040023.

Sandrolini F., Franzoni E., Cuppini G., and Caggiati L. 2007. Materials decay and environmental attack in the Pio Palace at Carpi: A holistic approach for historical architectural surfaces conservation. *Building and Environment*, 42(5), 1966-1974.

Powers T.C. and Helmuth R.A. 1953. Theory of volume changes in hardened Portland-cement paste during freezing. *In: Proceedings, Highway Research Broad Annual Meeting, National Academy of Science*, 285-297.

Roels S., Carmeliet J., Hens H., Adan O., Brocken H., Černý R, et al. 2004. Interlaboratory comparison of hygric properties of porous building materials. *Journal of Thermal Envelope and Building Science*, 27, 307–325.